JOURNAL OF ENGINEERING AND APPLIED SCIENCE, VOL. 48, NO. 2, APR. 2001, PP. 263-279
FACULTY OF ENGINEERING, CAIRO UNIVERSITY

UTILIZING ARTIFICIAL NEURAL NETWORKS FOR PREDICTING SHORELINE CHANGES BEHIND OFFSHORE BREAKWATERS

H. A. A. REFAAT[1]

ABSTRACT

The shoreline changes in the vicinity of offshore breakwaters are significantly influenced by the geometric parameters of offshore breakwaters. The complexity of the behaviour of shoreline changes behind offshore breakwaters makes it difficult to predict analytically these changes. As a result, numerical models are frequently used. In this paper, Artificial Neural Networks (ANNs) are developed to predict the shoreline changes behind offshore breakwaters. The developed ANN models can accurately predict the salient size, X_S , the sand deposited volume behind offshore breakwaters, V_S , for a known set of geometric parameters of offshore breakwaters. Four geometric parameters are found to be important, they are: the breakwater length, L_B, the offshore distance of the breakwater from the original shoreline, X_B, the surf zone width, X_b and the gape spacing between adjacent breakwaters, G_B, respectively. A comparison between ANNs and regression models for predicting the salient size and sand deposited volume is presented and the advantages of utilizing ANN methodology over regression techniques in model development are highlighted.

KEYWORDS: Neural networks, offshore breakwaters, beach protection, salient size, sand deposited volume.

1. INTRODUCTION

The use of offshore breakwaters for beach protection has increased substantially in the last two decades. They are generally constructed away from and parallel to the shoreline to dissipate wave energy and cause sand deposition in the sheltered area behind the breakwater. Although numerous field observations and physical models

[1] Associate Professor, Irrigation and Hydraulics Department, Faculty of Engineering, Cairo University

have been conducted to study the phenomenon, the complicated hydrodynamics and sediment transport mechanism around the breakwater have not been fully understood.

It is known that the currents engendered behind the breakwater by wave dissipation in the sheltered area are building a new equilibrium shape of the shoreline. This new shoreline is affected by many parameters, including sediment supply, sediment properties, wave characteristics, coastal zone topography and breakwater configuration, see Fig. 1. However, the most pronounced parameters appear to be: the breakwater length, L_B , the offshore distance of the breakwater from the original shoreline, X_B , the surf zone width, X_b and the gap spacing between adjacent breakwaters, G_B. The contributions of these parameters to salient size and sand deposited volume is difficult to model physically since all of these parameters mutually interact and the relationships between them are not well understood.

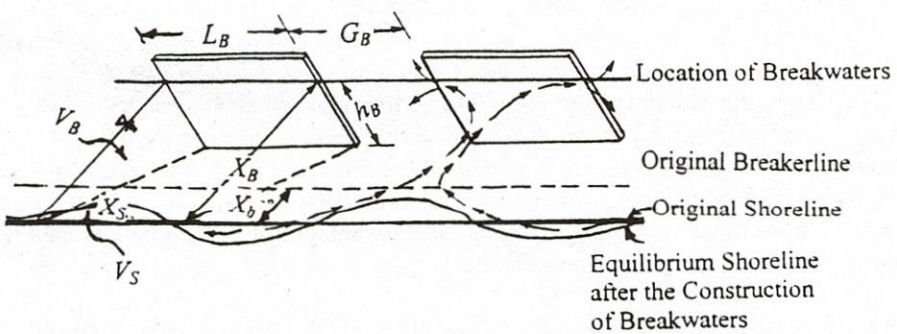

Fig. 1. Schematic diagram of offshore breakwaters.

This paper describes an effort to predict the salient size and sand deposited volume behind offshore breakwaters, using the technique of Artificial Neural Networks (ANNs). Neural networks provide a non-parametric and model-free mapping between a given set of input data and that of output data. Details of the theoretical concepts involved in ANNs can be found in any of the standard textbooks [1,2]. Applications of neural networks in civil engineering are relatively recent [3-6] and include a variety of coastal problems such as: forecasting wave height

interpolations for shorter duration, given their observations over longer periods [7], tidal-level forecasting [8], stability analysis of rubble-mound breakwaters [9], and prediction model for occurrence of impact wave force [10].

2. ANALYZED DATA

Many coastal engineers have tried to find the proper design criteria for an offshore breakwater system relating its geometric parameters to the corresponding shoreline change by means of physical model test [11-15], numerical modeling [16,17], or the investigation of the previously constructed offshore breakwater systems [18-21].

For the purpose of developing an ANN model to predict accurately shoreline changes behind offshore breakwaters, represented by salient size and sand deposited volume, it is important to develop an understanding of the dimensional analysis of the governmental parameters. The functional relationships of the governing parameters for shoreline changes behind offshore breakwaters can be written in the dimensionless from as:

$$\frac{X_S}{X_B}\cdot\frac{V_S}{V_B} = f\left(\frac{L_B}{gT^2}\cdot\frac{L_B}{X_B}\cdot\frac{X_b}{X_B}\cdot K_t\cdot\frac{G_B}{X_B}\cdot\frac{G_B}{L_B+G_B}\cdot\frac{Q_n}{H_b^3/T}\cdot\frac{V_f T}{H_b}\cdot\frac{D_{50}}{h_B}\right) \qquad (1)$$

where X_S is the distance to the end of the salient from original shoreline, h_B is the water depth at breakwater, H_b is the breaking wave height, T is the wave period, g is the acceleration of gravity, V_S is the deposited sand volume behind breakwater, V_B is the sheltered volume ($V_B = L_B X_B h_B/2$), Q_n is the longshore transport rate, K_t is the dimensionless wave transmission coefficient, D_{50} is the mean diameter of sediment grain, and V_f is the fall velocity of sediment.

It is obvious that the number of possible significant variables makes the design and analysis of data very difficult, and that if limited data are to be arranged in some meaningful way, certain assumptions must be made in order to reduce the number of variables. Due to the limitation in collecting and measuring field and experimental data, some variable will be eliminated and Eq. (1) will be reduced as:

- For measuring physical data

$$\frac{X_S}{X_B}, \frac{V_S}{V_B} = f\left(\frac{L_B}{gT^2}, \frac{L_B}{X_B}, \frac{X_b}{X_B}, \frac{V_f T}{H_b}\right) \tag{2}$$

- For collecting field data

$$\frac{X_S}{X_B}, \frac{V_S}{V_B} = f\left(\frac{L_B}{X_B}, \frac{G_B}{X_B}, \frac{G_B}{L_B + G_B}\right) \tag{3}$$

The available data from physical model studies are summarized in Table 1. All the data in the table are for single offshore breakwater subject to normal incident waves. Additionally, the summary of the characteristics of the offshore breakwaters in the field is presented in Table 2.

Table 1. Database of physical models.

Author	L_B/gT^2	L_B/X_B	X_b/X_B	V_fT/H_b	X_S/X_B	V_S/V_B
Shinohara and	0.180	2.000	2.133	0.500	0.360	0.630
Tsubaki (1966)	0.180	1.000	1.067	0.500	0.207	0.151
	0.180	0.566	0.604	0.500	0.132	0.051
	0.180	0.400	0.427	0.500	0.088	0.022
	0.180	2.000	2.133	0.500	0.667	1.000
	0.180	1.000	1.067	0.500	0.387	0.400
	0.180	0.566	0.604	0.500	0.155	0.122
	0.180	0.400	0.427	0.500	0.053	0.022
Rosen and	0.080	0.167	0.453	0.870	0.053	0.011
Vajda (1982)	0.160	0.333	0.453	0.870	0.087	0.030
	0.320	0.667	0.453	0.870	0.127	0.065
	0.080	0.250	0.680	0.870	0.105	0.044
	0.080	0.500	1.360	0.870	0.240	0.230
	0.160	1.000	1.360	0.870	0.560	1.000
	0.320	2.000	1.360	0.870	0.820	1.000
	0.100	0.400	0.680	0.665	0.140	0.078
	0.050	0.250	0.850	0.665	0.115	0.053
	0.100	0.500	0.850	0.665	0.210	0.176
	0.200	1.000	0.850	0.665	0.330	0.436
	0.050	0.500	1.700	0.665	0.260	0.270
	0.100	1.000	1.700	0.665	0.550	1.000
	0.200	2.000	1.700	0.665	1.000	1.000
	0.050	0.500	1.700	0.665	0.250	0.250
	0.039	0.250	0.500	1.068	0.025	0.003
	0.077	0.500	0.500	1.068	0.120	0.058
	0.154	1.000	0.500	1.068	0.115	0.053

Author	L_B/gT^2	L_B/X_B	X_b/X_B	V_fT/H_b	X_S/X_B	V_S/V_B
Mimura, et al	0.189	0.833	1.000	0.295	0.361	0.573
Harris and	0.069	1.429	1.072	1.014	0.197	0.619
Herbich (1986)	0.069	1.429	1.072	1.014	0.204	0.667
	0.069	1.429	1.072	1.014	0.208	0.692
	0.069	1.000	0.596	1.014	0.166	0.439
	0.069	1.000	0.596	1.014	0.164	0.432
	0.069	0.800	0.680	1.014	0.109	0.190
	0.069	0.800	0.801	1.014	0.116	0.217
	0.069	0.800	0.425	1.014	0.127	0.257
Suh and	0.011	0.500	0.667	2.062	0.100	0.098
Dalrymple	0.032	1.500	0.667	2.062	0.867	0.759
(1987)	0.043	2.000	0.667	2.062	0.867	0.801
	0.053	2.500	0.667	2.062	0.767	0.640
	0.064	3.000	0.667	2.062	1.000	0.900
	0.043	1.500	0.500	2.062	0.225	0.280
	0.057	2.000	0.500	2.062	0.725	0.518
	0.071	2.500	0.500	2.062	0.500	0.610
	0.142	5.000	0.500	2.062	0.450	0.280
	0.071	2.000	0.400	2.062	0.300	0.260
	0.089	2.500	0.400	2.062	0.440	0.270
	0.106	3.000	0.400	2.062	0.420	0.240
	0.071	2.500	0.500	2.062	0.400	0.340
	0.071	2.500	0.500	2.062	0.675	0.470
	0.071	2.500	0.500	2.062	0.400	0.250
Ming and	0.127	1.500	0.833	0.676	1.000	0.667
Chiew (2000)	0.169	2.000	0.833	0.676	1.000	0.961
	0.212	2.500	0.833	0.676	1.000	0.859
	0.085	0.667	0.556	0.760	0.267	0.102
	0.127	1.000	0.556	0.760	0.693	0.518
	0.169	1.333	0.556	0.760	1.000	0.669
	0.212	1.667	0.556	0.760	1.000	0.619
	0.085	0.500	0.417	0.811	0.100	0.012
	0.127	0.750	0.417	0.811	0.417	0.146
	0.169	1.000	0.417	0.811	0.670	0.413
	0.212	1.250	0.417	0.811	1.000	0.517
	0.085	0.400	0.333	0.845	0.027	0.001
	0.127	0.600	0.333	0.845	0.227	0.047
	0.169	0.800	0.333	0.845	0.400	0.160
	0.212	1.000	0.333	0.845	0.627	0.404
	0.077	2.000	1.000	0.914	1.000	0.693
	0.077	0.714	0.357	1.164	0.400	0.104
	0.077	0.714	0.357	1.164	0.371	0.107

Table 2. Database of field observations.

Author	L_B/X_B	G_B/X_B	G_B/L_B+G_B	X_S/X_B	V_S/V_B
Fried (1976)	1.111	0.519	0.318	1.000	0.419
	1.035	0.560	0.351	1.000	0.469
	1.077	0.538	0.333	1.000	0.441
	1.550	0.750	0.326	1.000	0.363
	1.200	0.750	0.385	1.000	0.208
	1.375	0.750	0.353	1.000	0.296
Toyoshima (1982)	1.364	0.455	0.250	1.000	0.868
	1.364	0.455	0.250	1.000	1.183
	1.035	0.345	0.250	0.778	0.374
	1.500	0.500	0.250	1.000	1.200
	1.071	0.357	0.250	1.000	0.600
	1.500	0.500	0.250	1.000	0.771
	0.968	0.323	0.250	0.768	0.711
	1.304	0.435	0.250	1.000	0.710
	1.500	0.500	0.250	1.000	0.596
	2.000	0.667	0.250	1.000	1.677
	2.000	0.667	0.250	0.480	0.526
	1.351	0.451	0.250	0.919	0.819
Dally and	0.889	2.000	0.692	0.689	0.475
Pope (1986)	0.667	1.250	0.652	0.200	0.040
	0.667	1.000	0.600	0.100	0.010
	0.727	1.364	0.652	0.291	0.085
	0.923	0.692	0.429	0.939	0.881
	0.923	0.692	0.429	0.954	0.910
	0.923	0.692	0.429	0.908	0.824
	0.923	0.692	0.429	0.939	0.881
	0.923	0.692	0.429	0.939	0.881
	3.750	1.667	0.308	1.000	1.000
	2.500	1.375	0.355	0.583	0.340
	2.500	1.083	0.302	0.333	0.111
	2.917	0.320	1.375	0.625	0.391

3. ARTIFICIAL NEURAL NETWORKS

In recent years, there has been a growing interest in a class of computing devices that operate in a manner analogous to that of biological nervous system. These devices, known as Artificial Neural Networks (ANNs), are finding applications in almost all branches of science and engineering.

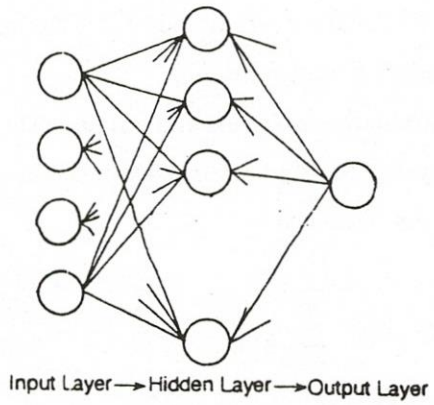

Fig. 2. Three layered ANN.

The emergence of ANN scheme was driven by the present understanding of how the neuronal architecture and operation of the human brain might function. Because of the similarity of ANNs fundamental model to that of human brain, ANNs have some unique human-like capabilities in information processing. ANNs do not have to be programmed to solve a problem, they learn from examples, which is the most important capability of ANNs. ANNs are capable of learning complex, highly nonlinear relationships and association of limited data.

The Information and knowledge learned by the ANNs is encoded and stored in the connection weights of the network. The retrieval of the stored information is done routinely by providing the network with an input pattern, which acts as a key. Once the learning is done, ANNs can give reasonable answers to the problem and use them in recall as many times as desired. As shown in Fig. 2 the topology of ANN consists of three layers; input layer, hidden layer and output layer. The three layers are connected with connections represented by the weight matrices and its biases. An algorithm, known as the error back-propagation algorithm [1, 2], was chosen to perform the procedure as follows:

1- **Initialize weights and biases:** All input and output values were normalized, and all weights V_{ik} and W_{kj}, and their biases were initialized by a random number within the interval (-1, 1); where V_{ik} is the weight matrix between the i^{th} input

neuron and the k^{th} hidden neuron; and W_{kj} is the weight matrix between the k^{th} hidden neuron and the j^{th} output neuron.

2- **Propagate the simulation of inputs and outputs:** The output H_k of the k^{th} hidden neuron, given by the log-sigmoid transfer function of the weighted sum of all inputs it received, is calculated by

$$H_k = \frac{1}{1 + exp(-\sum_{i=1}^{A} V_{ik} X_i)} \quad for \quad k = 1,2,\ldots\ldots\ldots\ldots, B \tag{4}$$

where A and B are total number of input neurons and total number of hidden neurons, respectively, and X_i is input value at the input neuron. The output Uj of the jth output neuron is similarly calculated:

$$U_j = \frac{1}{1 + exp(-\sum_{k=1}^{B} W_{kj} H_k)} \quad for \quad j = 1,2,\ldots\ldots\ldots\ldots, C \tag{5}$$

where C is total number of output neurons.

3- **Back-propagate errors:** Start at output neurons and work back to hidden neurons. During this backward pass, compare the output U_j with the target output T_j to minimize the error function:

$$E = \frac{1}{2} \sum_{j=1}^{C} (T_j - U_j)^2 \tag{6}$$

by the gradient steepest descent method, resulting in the increment ΔW_{kj} in the weight W_{kj} as follows:

$$\Delta W_{kj} = \eta \; U_j (1 - U_j)(T_j - U_j) H_k \tag{7}$$

where η is the learning rate or the step size. This is used to minimize the error function. For further learning, any n^{th} increment on the weight W_{kj}, i.e. ΔW^n_{kj} is given as a function of $(n\text{-}1)^{th}$ increment ΔW^{n-1}_{kj} by

$$\Delta W^n_{kj} = \eta \; U_j (1 - U_j)(T_j - U_j) H_k + \alpha \; \Delta W^{n-1}_{kj} \tag{8}$$

where α is the momentum factor. Similarly, the nth increment ΔV^n_{ik} in the weight V^n_{ik} between the i^{th} input neuron and the k^{th} hidden neuron is given as a function of

its $(n\text{-}1)^{th}$ increment ΔV^{n-1}_{ik} by

$$\Delta V^{n}_{ik} = \eta X_i H_k (1 - H_k) \sum_{j=1}^{C} U_j (1 - U_j)(T_j - U_j) W_{kj} + \alpha \Delta V^{n-1}_{kj} \quad (9)$$

4- **The weights of the connection** are modified iteratively using the leafing technique until the total mean square error becomes as low as 0.0001.

4. APPLICATION OF ANNs TO SHORELINE CHANGES

As a preliminary examination, the characteristics of the neural network are checked. After several trails the number of hiddin neurons is taken equal to 10.

4.1. Application to Physical Models

For physical models, four input parameters corresponding to the dimensionless variables representing geometry of breakwater placement, wave properties and sediment characteristics, L_B/gT^2, L_B/X_B, X_b/X_B and V_fT/H_b, are employed to predict the dimensionless variables representing salient size and sand deposited volume behind offshore breakwater, X_S/X_B and V_S/V_B, respectively.

The effect of each input parameter on the prediction of salient size and sand deposited volume are separately investigated in Figs. 3(a-d), where the comparisons between actual and predicted values of salient size and sand deposited volume are shown. From this figure it is obvious that a less agreement can be achieved between actual and predicted values of X_S/X_B and V_S/V_B when each parameter L_B/gT^2 and V_fT/H_b are separately investigated; whereas a good agreement between actual and predicted values of X_S/X_B and V_S/V_B when each parameter L_B/X_B and X_b/X_B are separately investigated. Therefore, both parameters L_B/X_B and X_b/X_B are seen to be important in the study of the shoreline changes behind offshore breakwaters.

Figure 4 shows the comparison between actual and predicted values of X_S/X_B and V_S/V_B when all the input parameters are employed. It can be seen from this figure that the agreement between the actual and predicted values of X_S/X_B and V_S/V_B is improved comparing to those in Fig. 3, in which the effect of each parameter is investigated separately.

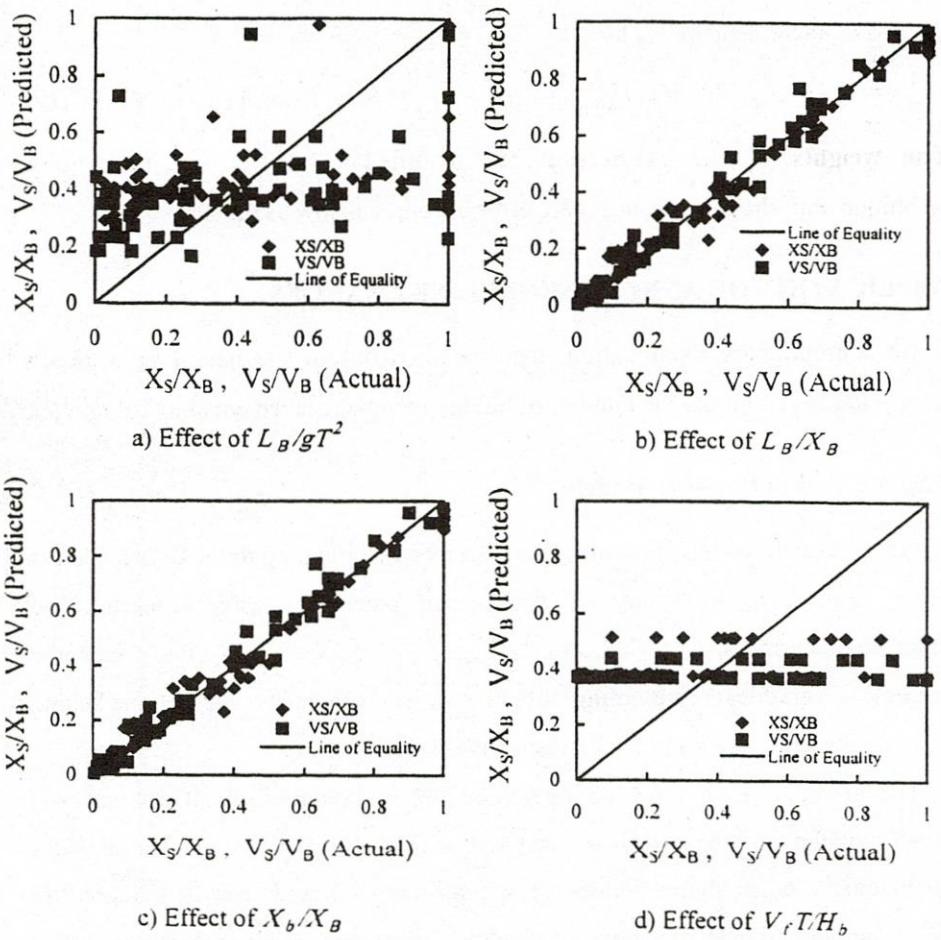

Fig. 3. Comparison between actual values of X_S/X_B and V_S/V_B measured in physical models and the predicted ones by ANNs when each parameters is investigated separately.

4.2. Application to field data

From available field data, three input parameters corresponding to geometry of breakwaters placement, in dimensionless form, L_B/X_B, G_B/X_B, G_B/L_B+G_B are employed to predict the dimensionless variable representing salient size and sand deposited volume behind offshore breakwaters, X_S/X_B and V_S/V_B , respectively. The effect of each input parameter on X_S/X_B and V_S/V_B is separately investigated in Fig. 5(a-c);

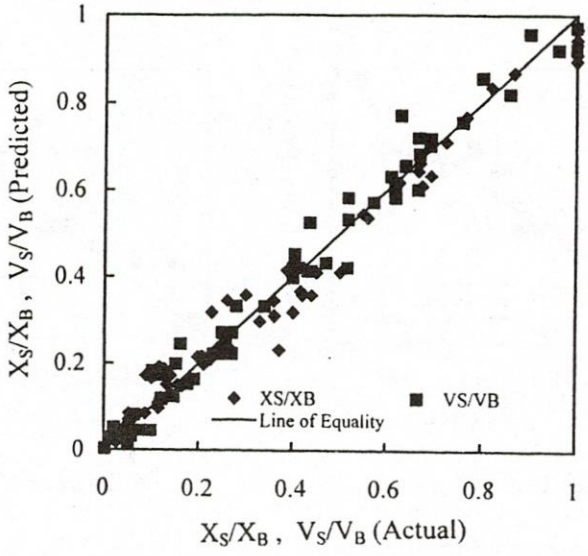

Fig. 4. Comparison between actual values of X_S/X_B and V_S/V_B measured in physical models and the predicted ones by ANNs when all the input parameters are employed.

where the actual and predicted values of X_S/X_B and V_S/V_B are shown. From this figure it is obvious that; the agreement between actual and predicted values of X_S/X_B and V_S/V_B is good when each input parameter L_B/X_B and G_B/X_B is separately investigated. A less agreement between actual and predicted values of X_S/X_B and V_S/V_B when the parameter G_B/L_B+G_B is separately investigated. This means that both parameters are seen to be important in the study of the shoreline changes behind offshore breakwaters.

Figure 6 shows the comparison between actual and predicted values of X_S/X_B and V_S/V_B when all the input parameters are used. It can be seen from this figure that the agreement between the actual and predicted values of X_S/X_B and V_S/V_B is improved comparing to those in Fig 5, in which the effect of each parameter is investigated separately.

5. ANNs VERSUS REGRESION MODELS

A comparison of ANNs with regression models is performed using two regression equations given by Suh and Dalrymple [17]; and Ming and Chiew[13].

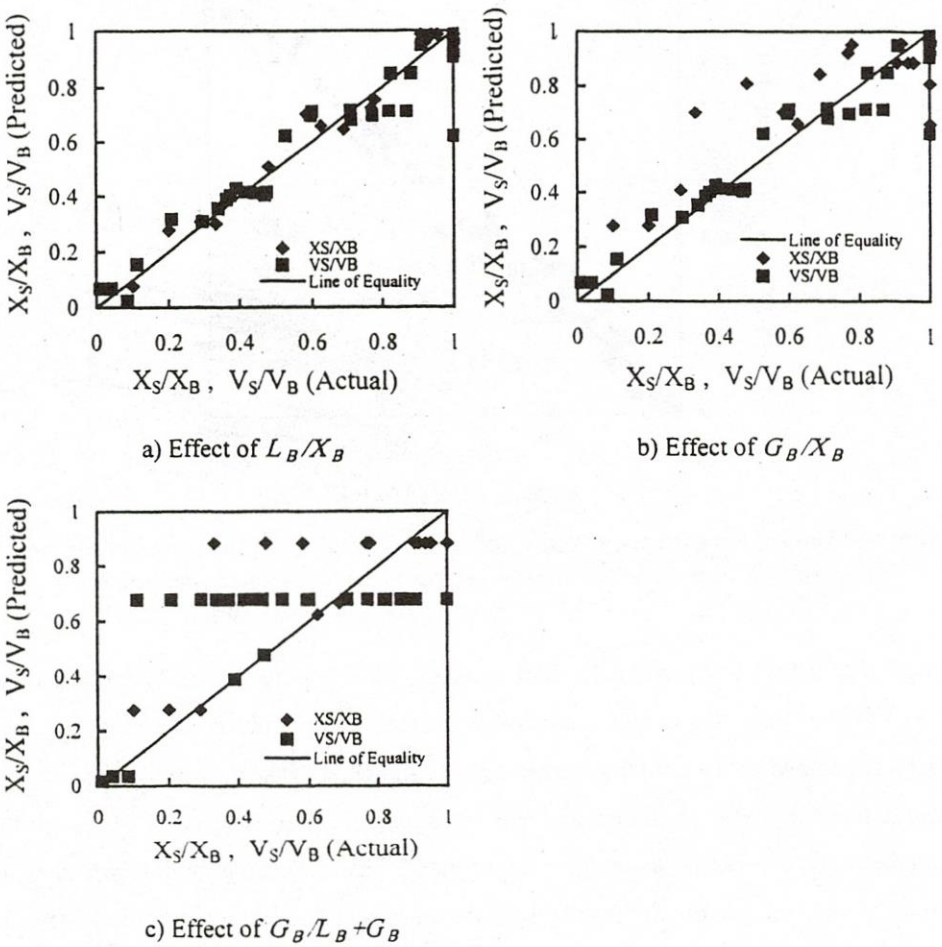

a) Effect of L_B/X_B

b) Effect of G_B/X_B

c) Effect of G_B/L_B+G_B

Fig. 5. Comparison between actual values of X_S/X_B and V_S/V_B measured in the field and the predicted ones by ANNs when each parameters is investigated separately.

The first equation was derived to estimate the salient size and the second one was derived to estimate the sand deposited area behind offshore breakwaters. Suh and Dalrymple [17] have derived their equation by using the approximately fitted curve for the available field data and is given by

$$\frac{X_S}{X_B} = 14.8\, A_1\, exp(-2.82\, A_1^{0.5}) \quad , \text{ where } \quad A_1 = \frac{G_B / X_B}{(L_B / X_B)^2} \tag{10}$$

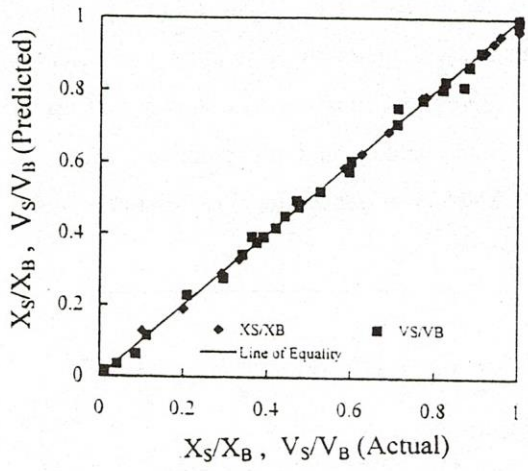

Fig. 6. Comparison between actual values of X_S/X_B and V_S/V_B measured in the field and the predicted ones by ANNs when all the input parameters are employed.

To perform a comparison between ANN model and Eq. (10), ANN was trained on the 22 sets and tested by 9 sets, where the development of any regression equation is usually based on utilizing all the data sets available, rather than leaving a subset for testing as it is commonly practiced with developing ANN. The values of X_S/X_B so predicted by ANN and regression equation are then compared with the actual values, as shown in Fig. 7. The ANN model has predicted the salient size with correlation coefficient = 0.9986 as compared to 0.7040 for the regression model.

Ming and Chiew [13] have derived their equation by using the approximately fitting curve for the experimental data and is given by

$$\frac{A_S}{X_B^2} = -0.384 + 0.043\frac{X_B}{L_B} + 0.711\frac{L_B}{X_B} \qquad (11)$$

where A_S is the deposited area. In order to perform a comparison between ANN model and regression equation, the deposited volume V_S was estimated using the deposited area A_S calculated from Eq. (11) as $V_S = A_S h_S$, where h_S is the beach height = $X_S \tan\beta$ and $\tan\beta$ is the beach slope. The ANN model was trained on the 53 sets and tested by 13 sets. The values of V_S/V_B so predicted by ANN model and regression equation are

compared with the actual values, as shown in Fig. 8. The ANN model has predicted the sand deposited volume with correlation coefficient = 0.9903 as compared to 0.7918 for the regression equation. As shown in Figs. 7 and 8, a close agreement between the actual values and the predicted values by ANNs may signify the effectiveness of ANNs over conventional regression models.

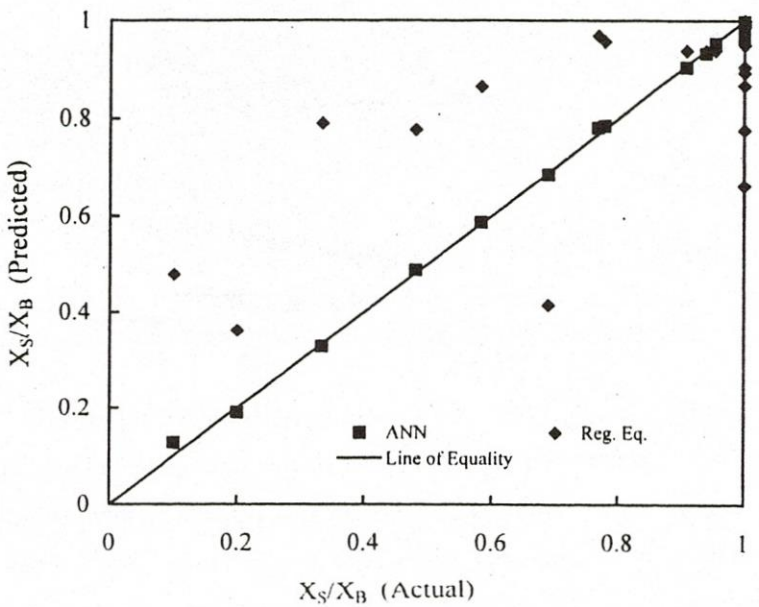

Fig. 7. Comparison between actual values of X_S/X_B and predicted ones by ANN and regression models.

6. CONCLUSIONS

Artificial neural networks (ANNs) based on the back-propagation algorithm were developed in this paper for predicting the shoreline changes behind offshore breakwaters. The use of ANNs was examined in terms of various design parameters of the breakwater configurations, sediment and wave characteristics. The developed ANN models can accurately predict the salient size and the sand deposited volume behind the breakwaters. The analysis of the ANN models show that the breakwater

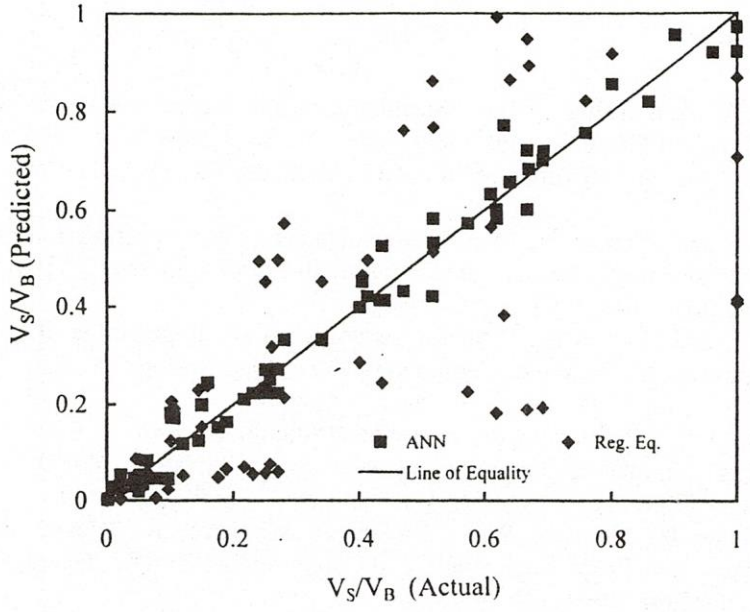

Fig. 8. Comparison between actual values of V_S/V_B and predicted ones by ANN and regression models.

length, L_B, the offshore distance of the breakwater from the original shoreline, X_B, the surf zone width, X_b and the gape spacing between adjacent breakwaters, G_B, appear to be important parameters that control the configuration of the shoreline shape and the amount of sand trapping behind the breakwaters.

The values predicted by ANNs were found to be more close to the actual values than those based on common regression models. This gives the advantage of using ANNs over regression models. Another advantage of the ANNs over regression models lies in their ability to model multi-output phenomena. Finally, ANNs do not have to be programmed to solve a problem, they learn from examples; once the learning is done, they can give reasonable answers to the problem and use them in recall as many times.

REFERENCES

1. Adedi, H., and Hung, S.L., "Machine Learing: Neural Networks, Genetic Algorithms and Fuzzy Systems", John Wiley and Sons, New York, 1995.
2. Wu, J.K., Neural Network and Simulation Methods, Marcal Dekker, New York, 1994.
3. Flood, I., and Kartam, N., "Neural Networks in Civil Engineering. I : Principles and Understanding", Journal of Computing in Civil Engineering, ASCE, Vol. 8, No. 2, pp. 131 – 148, 1994.
4. Flood, I., and Kartam, N., "Neural Networks in Civil Engineering. II : Systems and Application", Journal of Computing in Civil Engineering, ASCE, Vol. 8, No. 2, pp. 149 – 162, 1994.
5. Grubert, J.P., "Prediction of Estuarine Instabilities with Artificial Neural Networks", Journal of Computing in Civil Engineering, ASCE, Vol. 9, No. 4, pp. 266 – 274, 1995.
6. Karunanithi, N., Grenney, W.J., Whitley, D., and Bovee, K., "Neural Networks for River Flow Prediction", Journal of Computing in Civil Engineering, ASCE, Vol. 8, No. 2, pp. 201 – 221, 1994.
7. Deo, M.C., Rao, V.V. and Sakar, A., "Neural Networks for Wave Height Interpolation," Journal of Microcomputers in Civil Engineering, No. 12, pp. 217 – 225, 1997.
8. Tsai, C.P., and Lee, T.L., "Back-Propagation Neural Network in Tida-Level Forecasting," Journal of Waterway, Port, Coastal and Ocean Engineering, ASCE, Vol. 125, No., 4, pp. 195 – 202, 1999.
9. Mase, H., Sakamoto, M., and Sakai, T., "Neural Network for Stability Analysis of Rubble-Mound Breakwaters", Journal of Waterway, Port, Coastal and Ocean Engineering, ASCE, Vol. 121, No. 6, pp. 294 – 299, 1995.
10. Mase, H., and Kitamo, T., "Prediction Model for Occurrence of Impact Wave Force", Journal of Ocean Engineering, Elsevier Science Ltd., No. 26, pp. 949 – 961, 1999.
11. Harris, M.M., and Harbich, J.B., "Effects of Breakwater Spacing on Sand Entrapment", Journal of Hydraulis Research, Vol. 24, No. 5, pp. 347 – 357, 1986.
12. Horikawa, K., and Koizumi, C., "An Experimental Study on the Function of an Offshore Breakwater", 29th Annual Conference, Japanese Society of Civil Engineers, pp. 85 – 88, 1974.
13. Ming, D., and Chiew, Y.M., "Shoreline Changes Behind Detached Breakwater", Journal of Waterway, Port, Coastal, and Ocean Engineering, ASCE, Vol. 126, No. 2, pp. 63 – 70, 2000.
14. Rosen, D.S., and Vajda, M., "Sedimentological Influences of Detached Breakwaters", Proceedings of the 18th Coastal Engineering Conference, ASCE, Vol. 3, pp. 1930 – 1949, 1982.

15. Shinohara, K., and Tsubaki, T., "Model Study on the Change of Shoreline of Sandy Beach by the Offshore Breakwater", Proceedings of the 10th Coastal Engineering Conference, ASCE, Vol. 1, pp. 550 – 563, 1966.
16. Mimura, N., Shimizu, T., and Horikawa, K., "Laboratory Study on the Influence of Detached Breakwater on Coastal Change", Proceedings of Coastal Structures' 83, ASCE, Vol. 2, pp. 940 – 752, 1983.
17. Suh, K., and Dalrumple, R.A., "Offshore Breakwaters in Laboratory and Field", Journal of Waterway, Port, Coastal, and Ocean Engineering, ASCE, Vol. 113, No. 2, pp. 105 – 121, 1987.
18. Dally, W.R. and Pope, J., "Detached Breakwaters for Shore Protection," Technical Report CERC – 86 – 1, U.S. Army Engineer Waterways Experiment Stations, Coastal Engineering Research Center, Vicksburg, Miss, 1986.
19. Fried, L., "Protection by Means of Offshore Breakwaters", Proceedings of the 15th Coastal Engineering Conference, ASCE, Vol. 2, pp. 1493 – 1512, 1976.
20. Nir, Y., "Offshore Artificial Structures and Their Influence on the Israel and Sinai Mediterranean Beaches", Proceedings of the 18th Coastal Engineering Conference, ASCE, Vol. 3, pp. 1837 – 1856, 1982.
21. Toyoshima, O., "Variation of Foreshore Due to Detached Breakwaters", Proceedings of the 18th Coastal Engineering Conference, ASCE, Vol. 3, pp. 1873–1892, 1982.

استخدام الشبكات العصبية فى استنتاج التغيرات الحادثة لخط الشاطئ خلف حواجز الأمواج المنفصلة

يهدف البحث إلى دراسة استخدام الشبكات العصبية فى استنتاج التغيرات الحادثة لخط الشاطئ خلف حواجز الأمواج المنفصلة، حيث تقوم هذه الحواجز بحماية الشواطئ عن طريق تقليل طاقة الأمواج خلفها مما يسبب ترسيب الرمال على الشاطئ وحدوث تغيرات لخط الشاطئ ويتحكم فى هذه التغيرات عدة عوامل أهمها: أطوال الحواجز المنفصلة والمسافات بينها، وبعدها عن خط الشاطئ، ووقوعها داخل أو خارج منطقة تكسير الأمواج. وتستطيع الشبكات العصبية استنتاج التغيرات الحادثة لخط الشاطئ وحجم الرمال المترسبة خلف حواجز الأمواج المنفصلة بدقة عالية تفوق النماذج الرياضية المستخدمة لنفس الغرض.